Reviewed research article

# Energy balance of Brúarjökull and circumstances leading to the August 2004 floods in the river Jökla, N-Vatnajökull

Sverrir Guðmundsson[1], Helgi Björnsson[1], Finnur Pálsson[1], and Hannes H. Haraldsson[2]

[1] *Institute of Earth Sciences, University of Iceland, Sturlugata 7, 101 Reykjavík*

[2] *National Power Company of Iceland*

sg@raunvis.hi.is

**Abstract** — *We describe the energy balance and melting of the Brúarjökull outlet glacier of the Vatnajökull ice cap and the exceptional circumstances leading to two extreme floods in August 2004 in the main river Jökla draining the glacier. The energy balance was estimated using observations from three automatic weather stations and energy balance maps produced for the entire outlet glacier. Runoff calculated from the energy balance data satisfactorily agreed with measured river discharge. The results show that the first flood was forced by intensive rain and the second by exceptionally warm and sunny weather accompanied by unusually low glacier surface albedo. The energy balance data were used to optimize and evaluate three different empirical models that correlate glacial melting with air temperature measured 2 m above a non-glaciated surface, 20 km away from the glacier front. The glacier's peak-runoff was satisfactorily predicted with empirical models incorporating theoretically calculated clear-sky irradiance, but overestimated with a model that uses only estimated degree-days on the glacier, scaled with two constants that differ for snow and firn/ice.*

## INTRODUCTION

Vatnajökull ice cap (Figure 1) is located close to the maritime southeastern coast of Iceland. The north-facing, gently sloping Brúarjökull (1550 km$^2$) is the largest outlet of the ice cap, ranging in elevation from 600 to 1550 m a.s.l with a mean equilibrium line close to 1200 m a.s.l. (Björnsson *et al.*, 1998). Jökla is the main river draining 1250 km$^2$ of Brúarjökull (Figure 1). Two exceptionally large flood events were observed in the river during the periods August 3–6 and 9–14, 2004. By applying the river discharge model AQUARIVER that uses air temperature and precipitation away from the glacier, Hólm and Sigurjónsson (2004) concluded that the first flood was caused by intensive rain whereas the second was related to high air temperature. In the present paper we discuss the generation of these floods based on meteorological measurements on the glacier. We present energy budget calculations for the glacier during the entire summer of 2004 and compare the result to the energy budget since 1996. We also compare the corresponding glacial melt in 2004 with the measured river discharge. This provides a detailed description of the energy fluxes during production of the floodwater and explains how the flood events are related to weather parameters, the glacier winter balance and the surface albedo. Finally, the energy budget calculations are used to evaluate three distinct empirical ablation models based on a regression to air temperature measured 2 m above a non-glaciated surface at Eyjabakkar 655 m a.s.l., located ∼20 km away from the glacier front (Figure 1).

## OBSERVATIONS

### River discharge and the August 2004 floods

Hourly values for the discharge of the river Jökla were measured at Brú á Jökuldal, ∼40 km from the glacier margin (Figure 1). The water draining towards the discharge gauge is accumulated from 1250 km$^2$ of

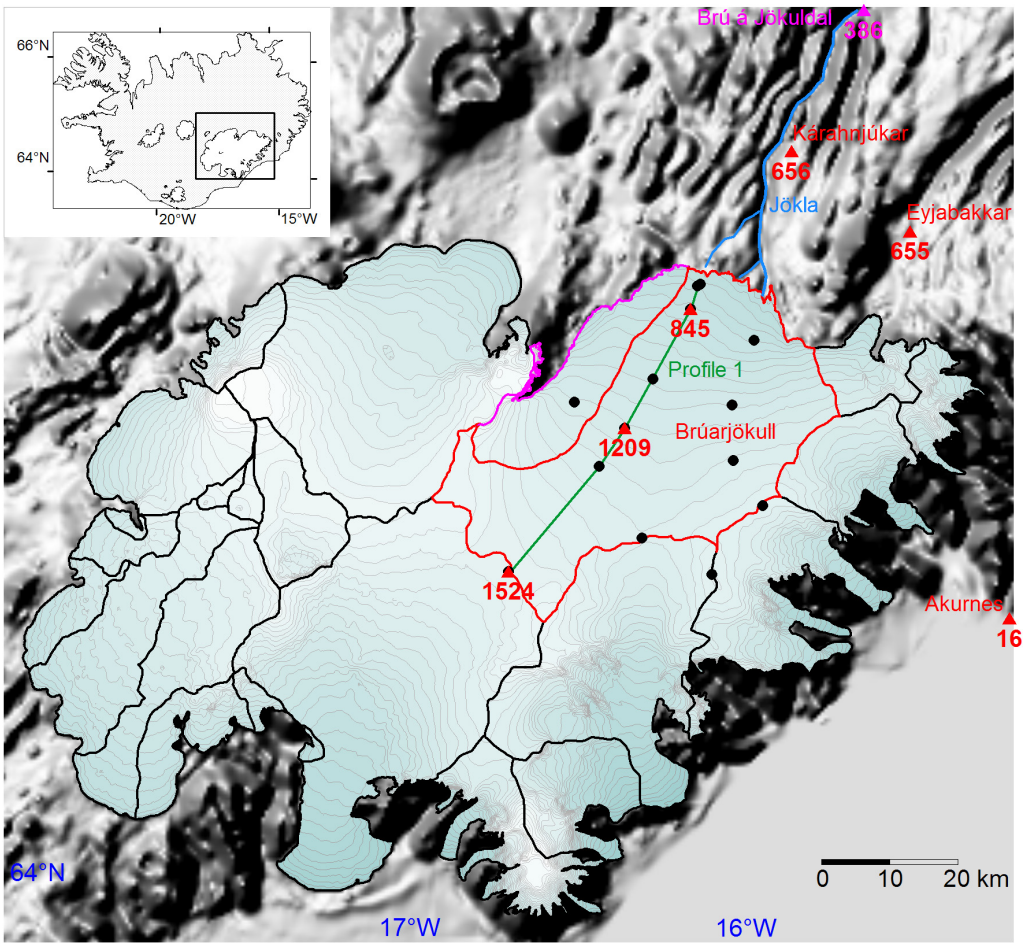



Figure 1. Study area and observation sites. Red and magenta outlines: Brúarjökull outlet glacier. Blue: the river Jökla. Red outline: the glaciated area of the water drainage basin of Jökla. Black dots: sites of the mass balance observations. Red triangles: meteorological stations on and away from the glacier and corresponding elevation in m a.s.l. Magenta triangle: location of the discharge gauge for Jökla. – *Vatnajökull og umhverfi hans, ásamt staðsetningu mælistika, sjálfvirkra veðurstöðva og rennslismælis fyrir Jöklu.*

glaciated and 632 km$^2$ non-glaciated areas. Located in the rain shadow north of Vatnajökull, most of the summer runoff at Brú á Jökuldal is glacial meltwater, about 80% on average and higher during days of high glacial runoff. The travel time of the river water from the glacier front to the discharge gauge is estimated at roughly 3 hours.

The first flood in Jökla during August 3–6 followed a period of intensive precipitation ($P_s$) observed from August 1-3 at Akurnes, ∼40 km southeast of Brúarjökull, but not at Kárahnjúkar, ∼20 km north of the outlet (Figure 2 and Table 1, see Figure 1 for location). Cloud cover visible on optical NOAA and MODIS satellite images indicates that the

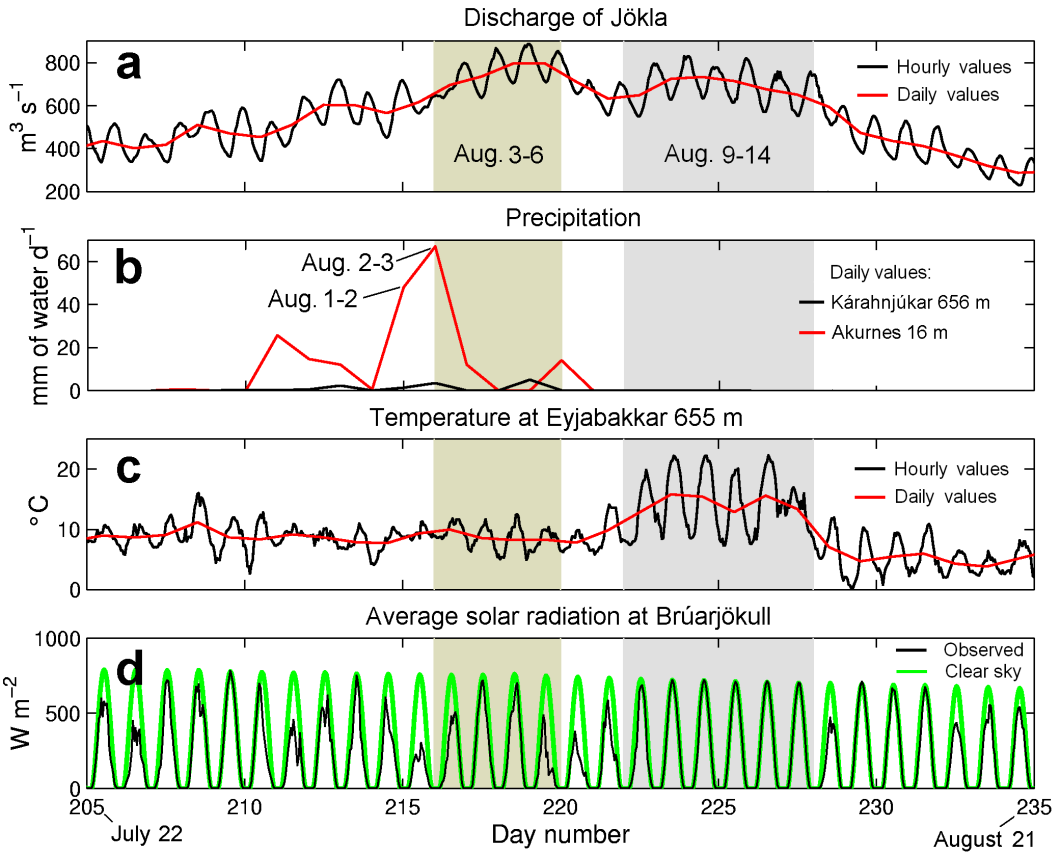



Figure 2. a) Discharge of Jökla observed at Brú á Jökuldal, 40 km north of the Brúarjökull terminus (Figure 1). b) Precipitation north and southeast of Brúarjökull. c) Temperature at Eyjabakkar 655 m. d) Measured solar radiation on Brúarjökull compared to theoretically calculated clear-sky irradiance (Olseth *et al.*, 1995). The floods occurred in two events: from August 3–6 and 9–14. The daily values of precipitation in (b) are accumulated from 9 am. GMT at day t to 9 am. GMT at day t+1, e.g. August 1–2 is from 9 am. on August 1 to 9 am on August 2 (see Table 1). Regular daily averages are used for the other parameters. – *Rennsli í Jöklu, úrkoma og lofthiti í veðurstöðvum utan Vatnajökuls og sólgeislun á Brúarjökli.*

heavy rainfall reached the glaciated area of the water drainage basin of Jökla (Einar Sveinbjörnsson, personal communication, 2005). The cyclonic weather system advanced first from the south during August 1–2, passing the highest parts of Brúarjökull, and then from the east during August 2–3, passing the entire outlet area. A rain shadow is clearly seen at the lowest elevations of Brúarjökull and north of the glacier on August 1–2, and north and northeast of the outlet on August 2–3. This can explain the low precipitation measured at Kárahnjúkar August 1–3 (Figure 2b). All this suggests that the rainfall peaked more or less within the glaciated area of the water drainage basin of Jökla (Figure 1). The second flood, from August 9–14, followed a period when exceptionally high air temperatures were observed at and around the outlet

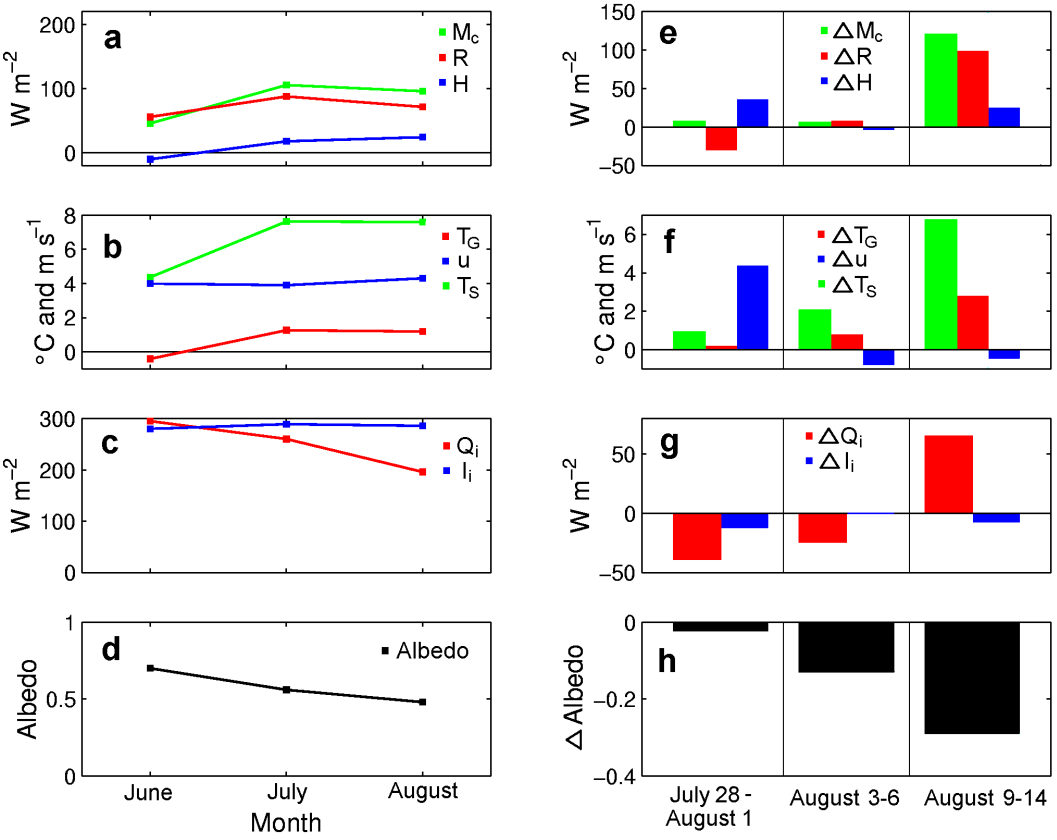



Figure 3. a-d) Monthly mean values (1996–2004) of meteorological parameters and energy fluxes at Brúarjökull (1200 m) and air temperature ($T_S$) observed away from the glacier at Eyjabakkar 655 m (Figure 1). e-h) Deviation of the July 28 to August 1, 2004 values from the July averages and August 3–6 and 9–14, 2004 values from the August averages. Parameters are defined on pages 124–125. – *Meðalmánaðargildi (1996–2004) veður- og orkuþátta á Brúarjökli, 1200 m y.s. og lofthita á Eyjabökkum, ásamt frávikum einstakra daga ársins 2004.*

glacier (Figures 2c and 3f). Furthermore, this was a period of unusually clear weather and hence high solar radiation (Figure 3g). Figure 2d shows that the measured solar radiation from August 9-14 follows almost perfectly the theoretically calculated clear-sky irradiance.

**Data from the glacier**

Since 1996, one to three automatic weather stations (AWSs) at Brúarjökull have been used to measure the incoming ($Q_i$) and outgoing ($Q_o$) solar radiation, incoming ($I_i$) and outgoing ($I_o$) long-wave radiation and wind direction (*WD*) at 2 m elevation above the surface and wind-speed ($u$), air temperature ($T_G$) and relative humidity ($r$) at one to four levels above the surface (vertical profiles). Daily surface changes due to melting were measured directly by a sonic echo sounder and observed snow density was used to calculate the corresponding ablation ($a_s$) in water equiv-

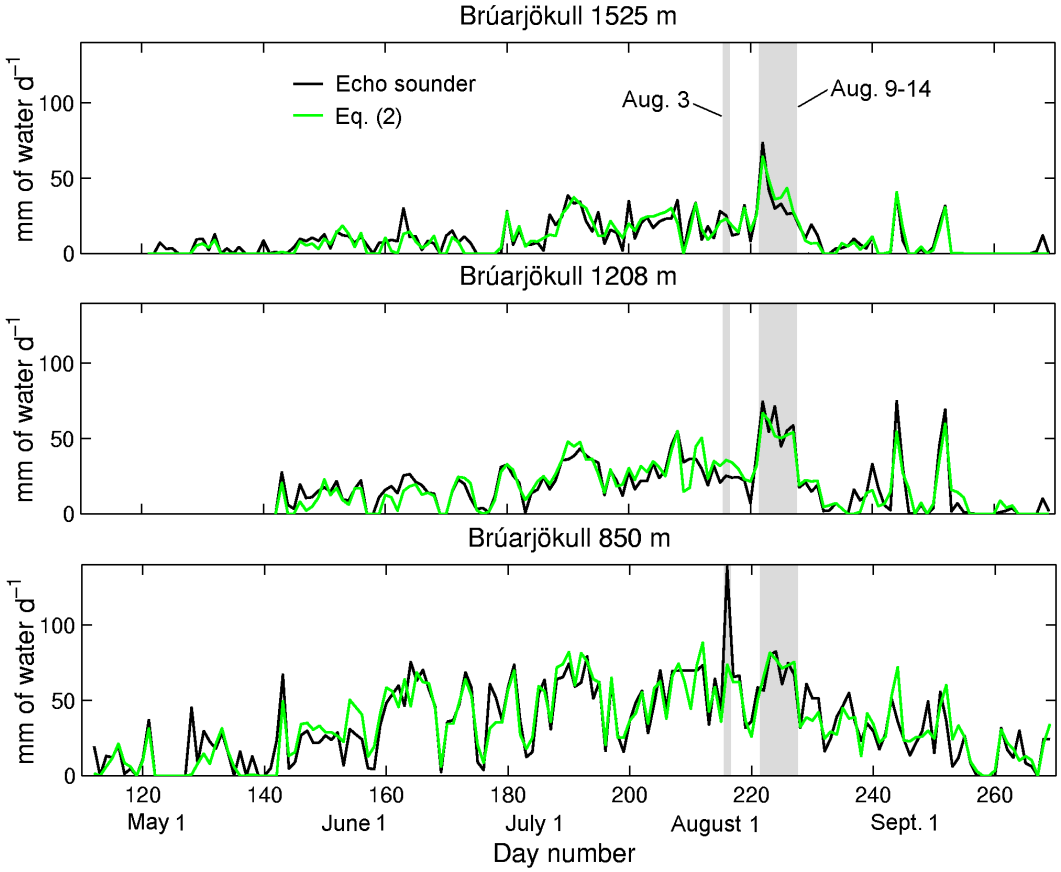



Figure 4. Measured and calculated daily melting at the three AWSs during the summer 2004. Black: direct measurement and green: calculated from the total energy supplied for melting. – *Mæld og reiknuð leysing í veðurstöðvum á Brúarjökli.*

alent. The total energy ($M_c$) for a melting glacier surface is expressed as

$$M_c = R + H + H_p\,, \tag{1}$$

where $R = Q_i - Q_o + I_i - I_o$ is the net radiation obtained from the observed radiation components and $H = H_d + H_l$ is the net turbulent heat flux calculated from the observed temperature, humidity and windspeed within the boundary layer; one- and two-level models with a stability factor (Monin and Obukhov method) were used to calculate the sensible ($H_d$) and latent ($H_l$) heat fluxes (e.g. Björnsson, 1972; Greuell and Genthon, 2003).

Heat supplied by precipitation ($H_p$) is considered negligible and the ablation calculated as

$$a_s = \begin{cases} \dfrac{M_c}{\rho L}; & M_c \geq 0 \\ 0; & M_c < 0 \end{cases}\,, \tag{2}$$

where $\rho = 10^3$ kg m$^{-3}$ is the density of water and $L = 3.3 \cdot 10^5$Jkg$^{-1}$ is the specific latent heat of melt-

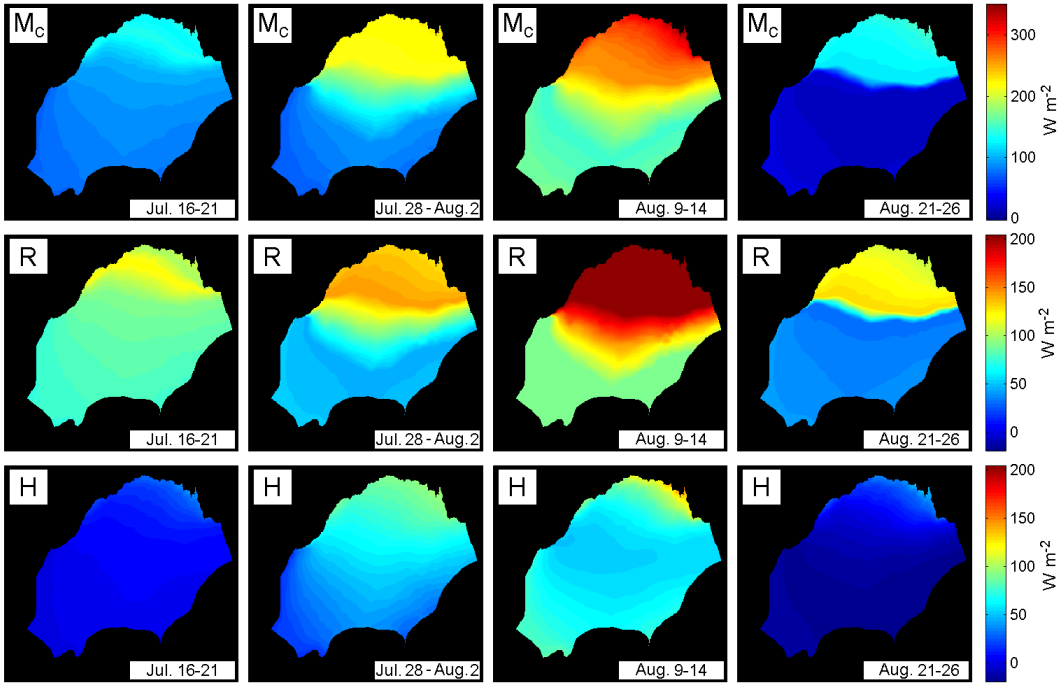



Figure 5. Energy budget maps averaged over six days. $M_C$: total energy supplied for melting as the sum of the net radiation ($R$) and the turbulent heat fluxes ($H$). – *Orkubúskapur á Brúarjökli.*

ing. Thus, $a_s$ was obtained by two independent methods: direct ablation measurements and energy budget calculations (Figure 4). A good consistency was obtained between calculated and measured melting, with a daily correlation of 0.91 at all the three stations.

Since 1992, measurements of annual summer ($b_s$) and winter ($b_w$) mass balance have been conducted at several points on Brúarjökull (Figure 1). Each year in April-May, cores for measuring winter mass balance and snow density have been drilled through the winter layer. The summer mass balance has been derived in September-October from readings at stakes and on wires that were drilled into the glacier in April or May and left there during the summer (Björnsson *et al.*, 1998, 2003). The AWS data, along with the measured $b_w$, was used to infer energy balance maps (EBMs) for the summer of 2004 (Figure 5). The weather parameters $T_G$, $r$, $u$, $Q_i$, and $I_i$ were assumed to vary only with elevation on the gently sloping outlet glacier (which is up to ∼53 km wide from east to west and ∼48 km long from north to south) and estimated for the whole outlet glacier by a linear interpolation between measurements at the three AWSs. The long-wave radiation emitted from the glacier surface ($I_o$) was taken as 315 Wm$^{-2}$ (from a melting surface) and the outgoing solar radiation as $Q_o = Q_i \cdot \alpha$. The observed albedo data (Figure 6) were used to infer changes in albedo ($\alpha$) for the whole outlet glacier when melting a) the winter snow ($b_w$), b) ice/firn after removal of the winter snow and c) snow that falls and melts during the ablation season.

The total ablation calculated from EBMs was generally consistent with the measured $b_s$ at the lower elevations, but considerably higher than measured at the two highest stakes (Figure 7a). This can be explained by frequent snowfall within the 2004 ablation

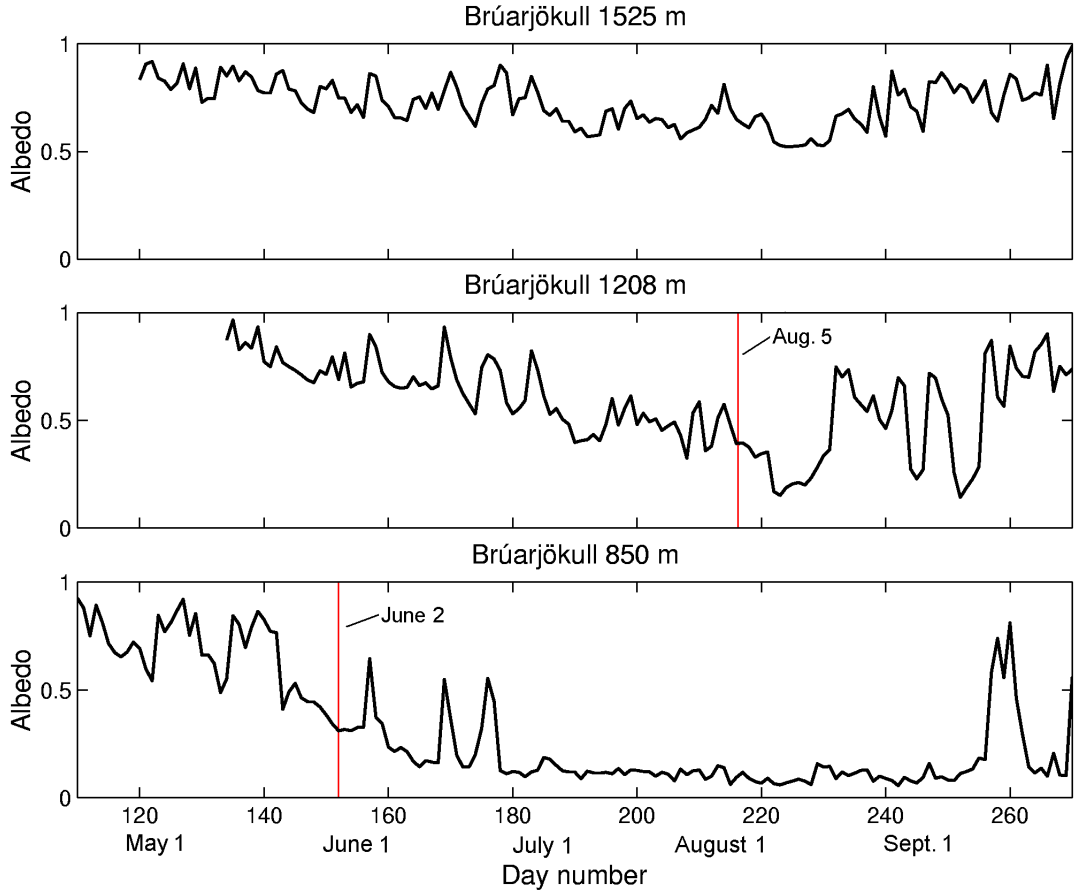



Figure 6. Daily values of albedo at the three AWSs (Figure. 1), estimated as the mean of the ratio $Q_o/Q_i$ between 13 to 14 pm GMT (during the time of day with the highest solar altitude). The red lines show days when the integrated melting equalled the observed winter accumulation (1449 and 283 mm of water at the 1208 and 850 m AWSs, respectively). The melting did not reach the previous year's summer surface at the highest elevation. – *Mældur endurkastsstuðull sólgeislunar í veðurstöðvum á Brúarjökli.*

season; snow that falls and melts within the summer is not detected by the reading of stakes at the end of the melting season, but the EBMs account for the energy supplied for melting the snow. The highly increased snowfall upglacier was clearly seen in the sonic echo sounder data at the AWSs. Furthermore, a similar discrepancy has been observed in other years at Brúarjökull, as well as at the other outlets of Vatnajökull and on the Langjökull ice cap located in SW Iceland (unpublished data). The deviation between the melting derived from the EBMs and the stake measurements is very low in general, or within 6% and 11% at all the stakes below 1000 and 1300 m a.s.l., respectively (Figure 7b). The measured summer balance was 0.75 and 0.50 m of water at the two highest stakes (at 1525 m), but 1.6 m derived from the energy bal-

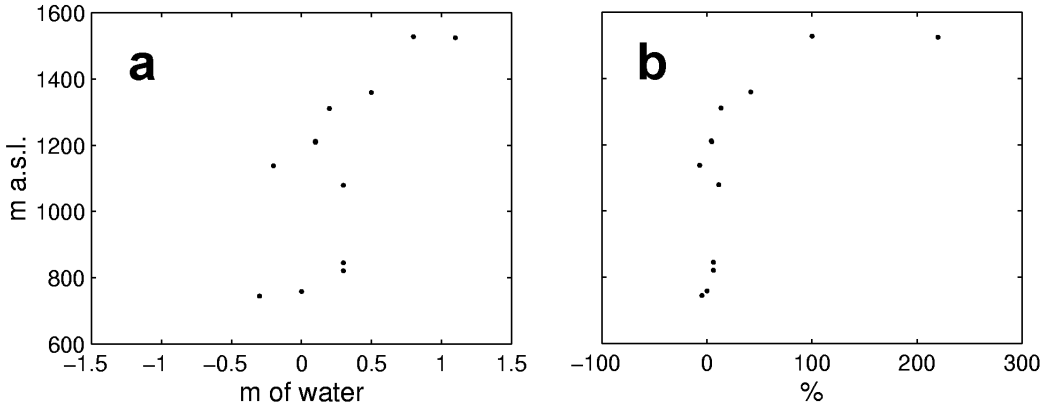



Figure 7. Deviation between the 2004 total summer melting calculated from the energy budget maps and the *in-situ* stake measurements of the summer balance, in m of water (a) and percent of the total melting (b); see Figure 1 for location of stakes. – *Munur á leysingu metinni útfrá orkubúskap annars vegar og aflestri á jöklastikum hins vegar.*

ance map. This deviation of ∼1 m of water is however close to the total summer accumulation measured by the sonic echo sounder at the 1525 m AWS.

## RESULTS

### Energy balance and weather parameters at the AWS sites

Annual variation in the average summer melting (June-August) during the period 1996–2004 is mainly caused by variation in net radiation ($R$), which is closely connected to the surface albedo and the previous year's winter mass balance ($b_w$), i.e. low $b_w$ tends to result in low albedo, and consequently a high $R$ (Figure 8a,c). Exceptions occurred during the summers 2002 and 2003 (Figure 8c). The mean summer values of the incoming solar ($Q_i$) and long-wave ($I_i$) radiation did not vary considerably from 1996–2004 (Figure 8d). The turbulent heat fluxes ($H$) closely follows the annual temperature ($T_G$) and wind-speed ($u$) variations (Figure 8a-b) observed within the downslope wind layer of the glacier (e.g. van den Broeke 1997; Oerlemans, 1998; Björnsson *et al.*, in press). For a melting glacier surface, the emitted long-wave radiation ($I_o$) is fixed at 315 Wm$^{-2}$, resulting in slightly negative net long-wave radiation balance (on average $I_i - I_o \approx -30$ Wm$^{-2}$) from June-August 1996–2004 (see $I_i$ in Figure 8d).

Mean values of energy, surface and weather parameters during the summer months for 1996–2004 are shown in Figure 3a-d; the station at the ELA (1200 m) is chosen as an example because it contains the longest time series on the glacier and has proven to be representative for the whole outlet.

Good consistency was obtained between the daily melting measured directly from a sonic echo sounder and that calculated with Eq. (2) (Figure 4) during the summer of 2004. Data for August 3 was, however, exceptional, with much higher melting measured at the lowest station by the sonic echo sounder than calculated with Eq. (2). If precipitation of 80 mm d$^{-1}$ is assumed, no more than 8% of this difference may be explained by heat supplied by precipitation ($H_p$) and 2% by frictional heat from water flowing everywhere on the surface of Brúarjökull. The difference might be explained by frictional heat if it is assumed that water flows in channels covering only 2–3% of the glacier surface. Thus, an extensive amount of water flowing in a channel formed below the sonic echo sounder is a possible explanation. The discrepancy could also

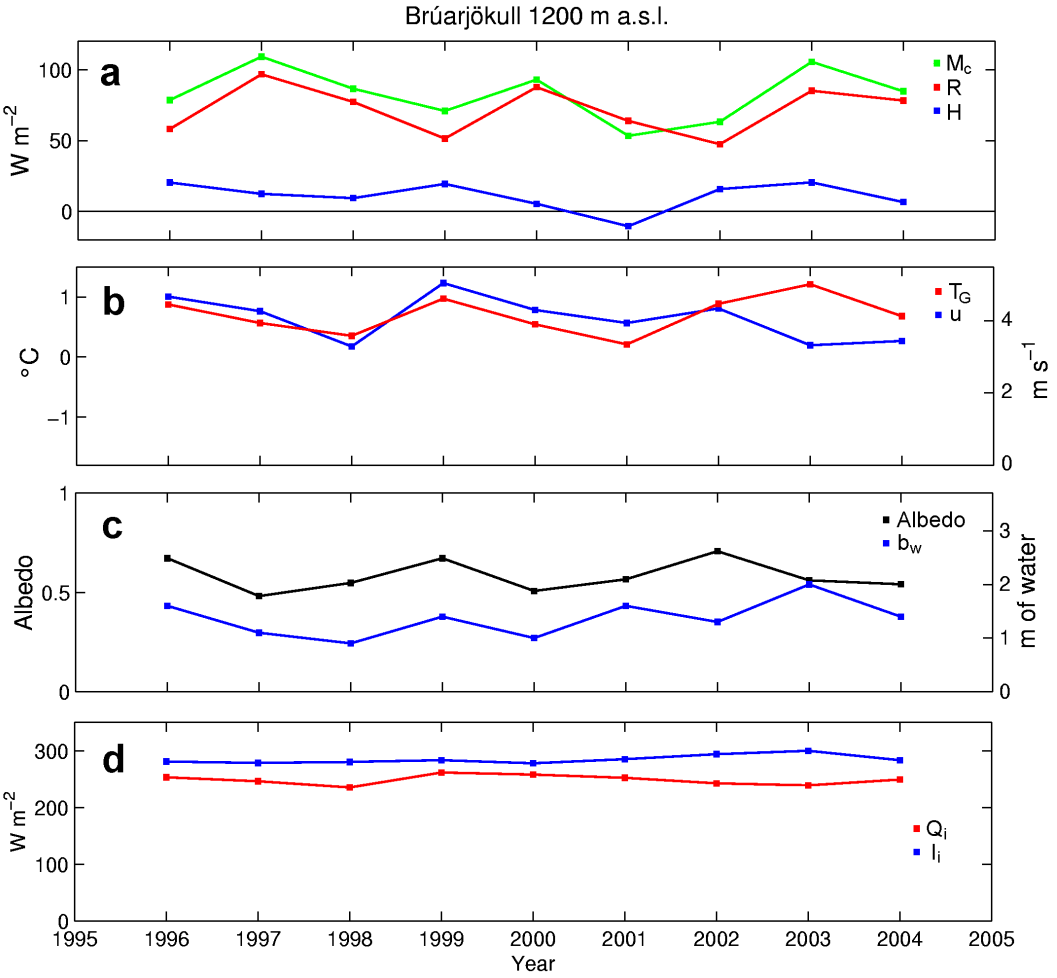



Figure 8. Mean summer values (June-August) at Brúarjökull 1200 m. a) Energy components supplied to melting. b) Temperature and wind-speed. c) Surface albedo and the specific balance of the previous winter (September-May). d) Incoming short- and long-wave radiation. Parameters are defined on p. 124–126. – *Árleg sumarmeðaltöl (júní-ágúst) veður- og orkuþátta á Brúarjökli, 1200 m y.s.*

be due to the intensive water flow flushing away fragments of the granular ice surface.

During the ablation season from the end of May to the end of September, the main contribution to melting was from net radiation (Figure 9); 77% at 950 m up to 92% at 1525 m, i.e. the smallest input from the net turbulent heat flux was in general at the highest site, where temperatures hovered around 0°C. Those numbers did, however, vary within the ablation season, e.g. during the period from July 28 to August 14 (days 210–227), when high temperatures and wind-speeds were frequently observed (Figure 10b), the contributions from the net turbulent heat flux were on average around 30% at the lowest and highest stations

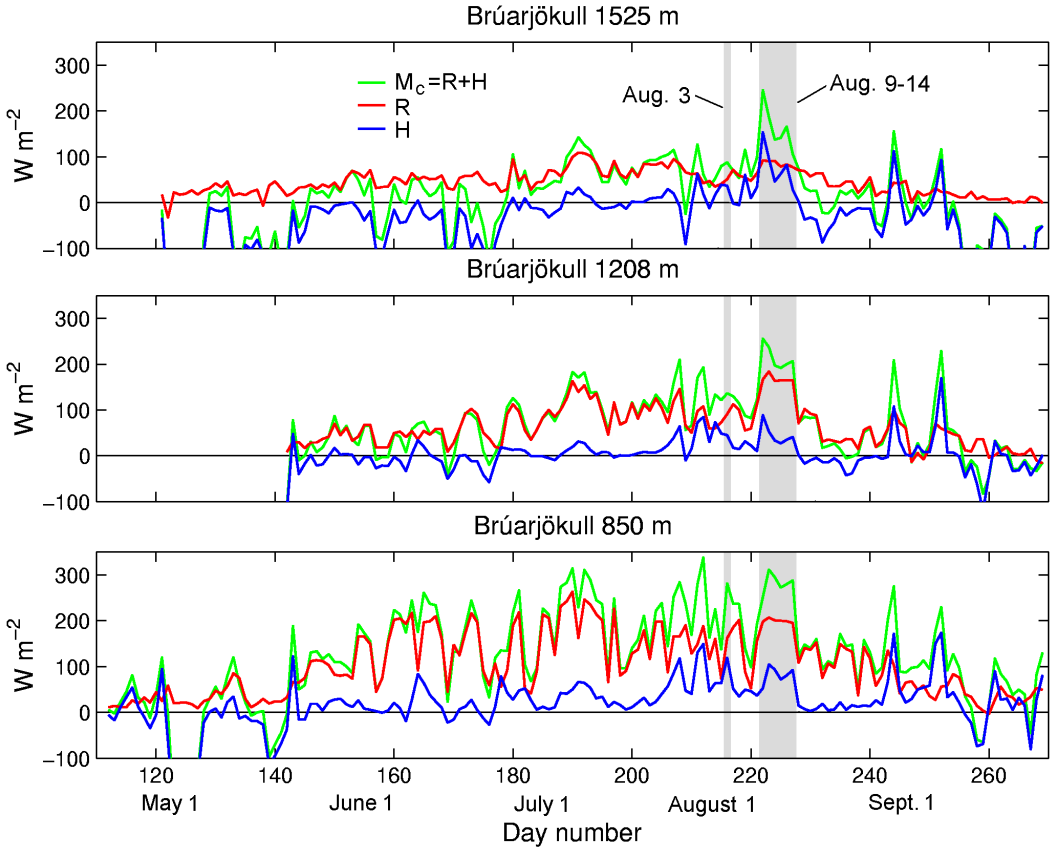



Figure 9. Daily energy balance at the three AWSs during the summer 2004. Parameters are defined on page 125. – *Orkuþættir í veðurstöðvum á Brúarjökli.*

(Figure 9) and up to 63% for single days at the highest station. About 90% of the daily variation in net radiation ($R$) was caused by the net short-wave radiation balance ($Q_i(1-\alpha)$), and the net turbulent heat flux were driven both by temperature and wind-speed; 97% of the daily variation in $H$ is described with $T_G{\cdot}u$ (Figure 10a,c,d).

High turbulent heat fluxes, driven by exceptionally strong southerly winds, were observed during the five days from July 28 to August 1 (Figures 3e,f and 10a,b). These heat fluxes, which were 34 $\mathrm{Wm}^{-2}$ above the July average (1996–2004), were partly counteracted by low solar radiation resulting in net radiation of 28 $\mathrm{Wm}^{-2}$ below the July average (Figure 3e,g). The wind-driven turbulent heat fluxes during those 5 days did, however, increase the melting and sped up the removal of snow in the ablation area of Brúarjökull.

A moderate August energy balance and melting was observed on Brúarjökull during the period of the first flood (Figure 3e). The intensive melting during the second flood was driven by both high turbulent heat fluxes and net radiation (Figures 4, 9 and 10). During that period, temperatures of 2.7°C and 6.7°C above the August average (1996–2004) were observed at 1200 m on the glacier and at Eyjabakkar 655 m

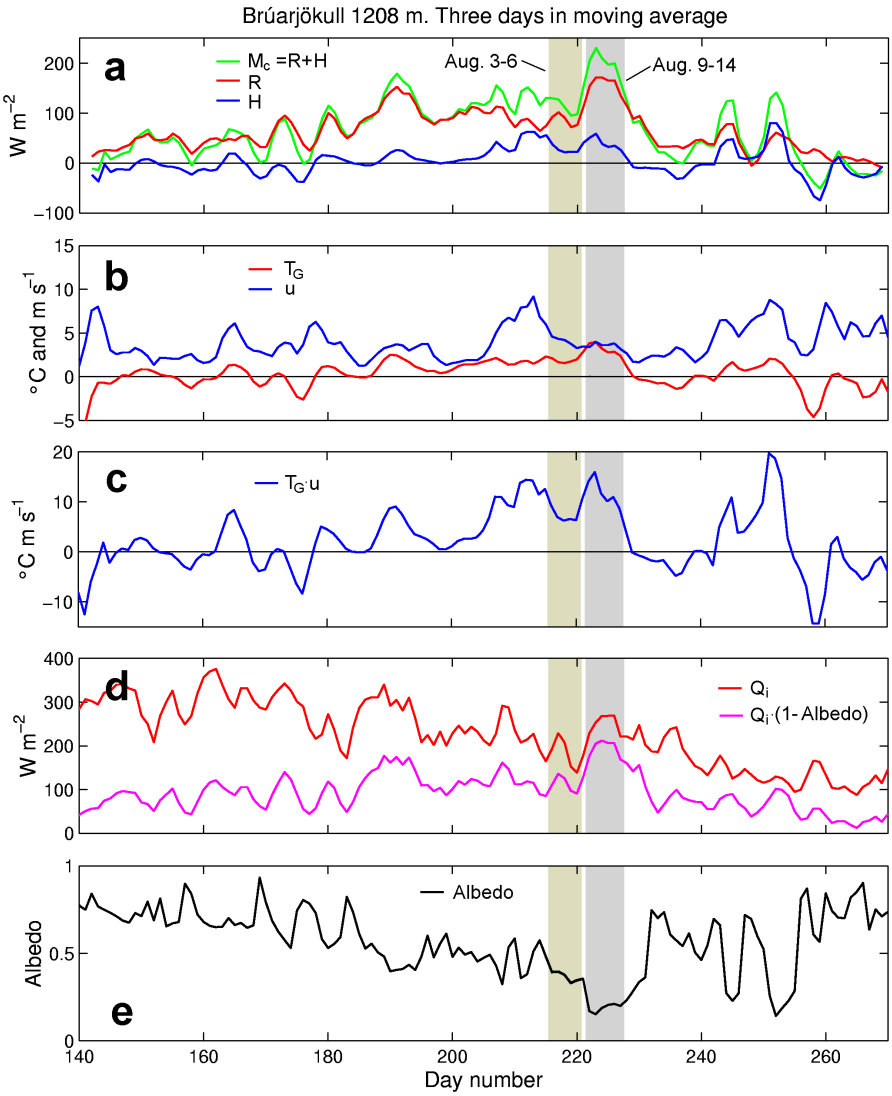



Figure 10. a) Energy balance. b-d) Weather parameters on the glacier. e) Surface albedo. Parameters are defined on p. 124–125. – *Veður- og orkuþættir á Brúarjökli, 1200 m y.s.*

respectively, resulting in a net turbulent heat flux of 91% above the August average (Figure 3e,f). According to weather data from the Icelandic Meteorological Office, this exceptionally warm air was advected from the southeast over Vatnajökull from an extensive high-pressure system stretching over the Atlantic Ocean to Mediterranean latitudes. The ocean acts as a reactor, cooling the air in the lowest layers of the atmosphere and during unusually warm days, temperature inversions are often observed around 1000 m a.s.l. (Einar Sveinbjörnsson, personal communication, 2005). This was measured by the AWSs at

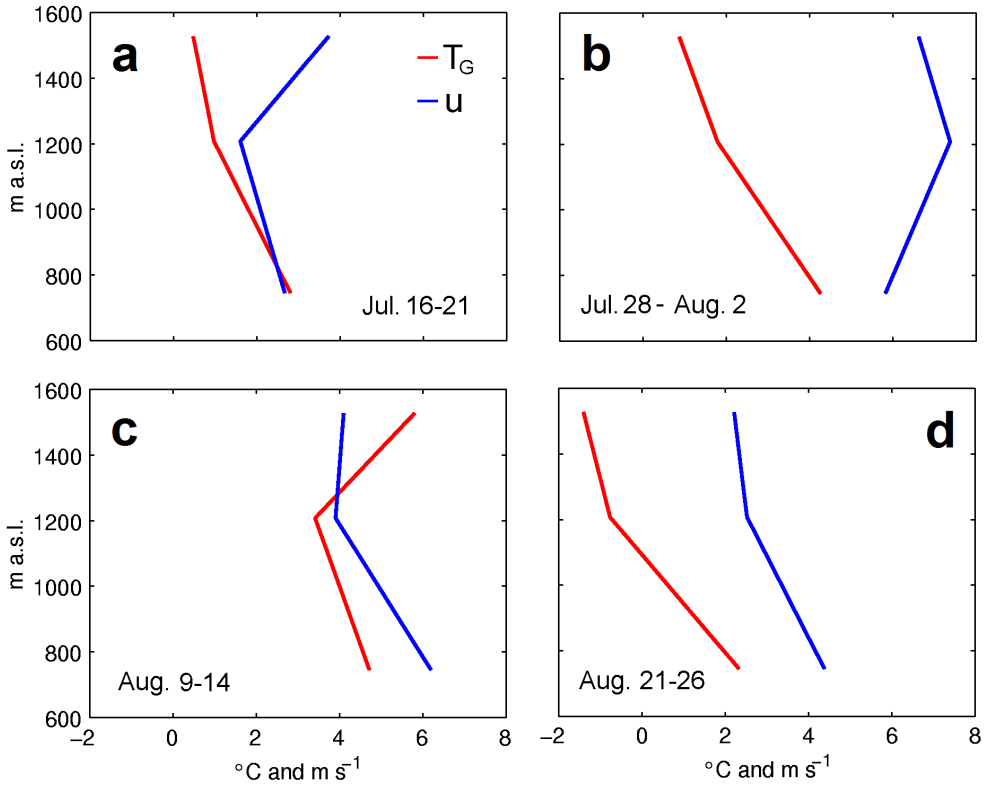



Figure 11. Six-day averages of air temperature ($T_G$) and wind-speed ($u$) along a longitudinal central profile on Brúarjökull (Profile 1 in Figure 1). Days displayed in (a-d) are the same as in Figure 5. – *Hita- og vindstigull milli veðurstöðva á Brúarjökli.*

Brúarjökull during the warm period from August 9-14 (Figure 11c). At the ELA, the high solar radiation during the period August 9-14 (Figure 3g) along with abrupt lowering in the albedo on August 9 (Figure 10e) resulted in net radiation 135% above the August average for 1996–2004 (Figure 3a). In all, the high energy fluxes during August 9-14 caused melting 124% above the August average at the 1200 m AWS (Figure 3e).

**Energy budget of Brúarjökull 2004**

The net radiation over the outlet increased as the snowline moved upglacier (R in Figure 5). The net turbulent fluxes followed the temperature and wind-speed changes (H in Figure 5 and Figure 11). The high solar radiation and low albedo during the period August 9–14 resulted in high net radiation over the whole Brúarjökull, although much more occurred below than above the snowline; ∼200 Wm$^{-2}$ below 1100 m a.s.l. and ∼90 Wm$^{-2}$ at the highest elevations (Figure 5). During that period, the high turbulent heat fluxes were driven by exceptionally high temperatures and strong, stable winds (Figures. 11c and 10b). The variation with elevation of the turbulent heat fluxes, from 110 Wm$^{-2}$ at the lowest elevation down to 50 Wm$^{-2}$ around the ELA (1200 m), and again up to 80 Wm$^{-2}$ at the highest elevations (Figure 5), is consistent with the air temperature gradient seen in Figure 11c. Both the high turbulent heat fluxes and

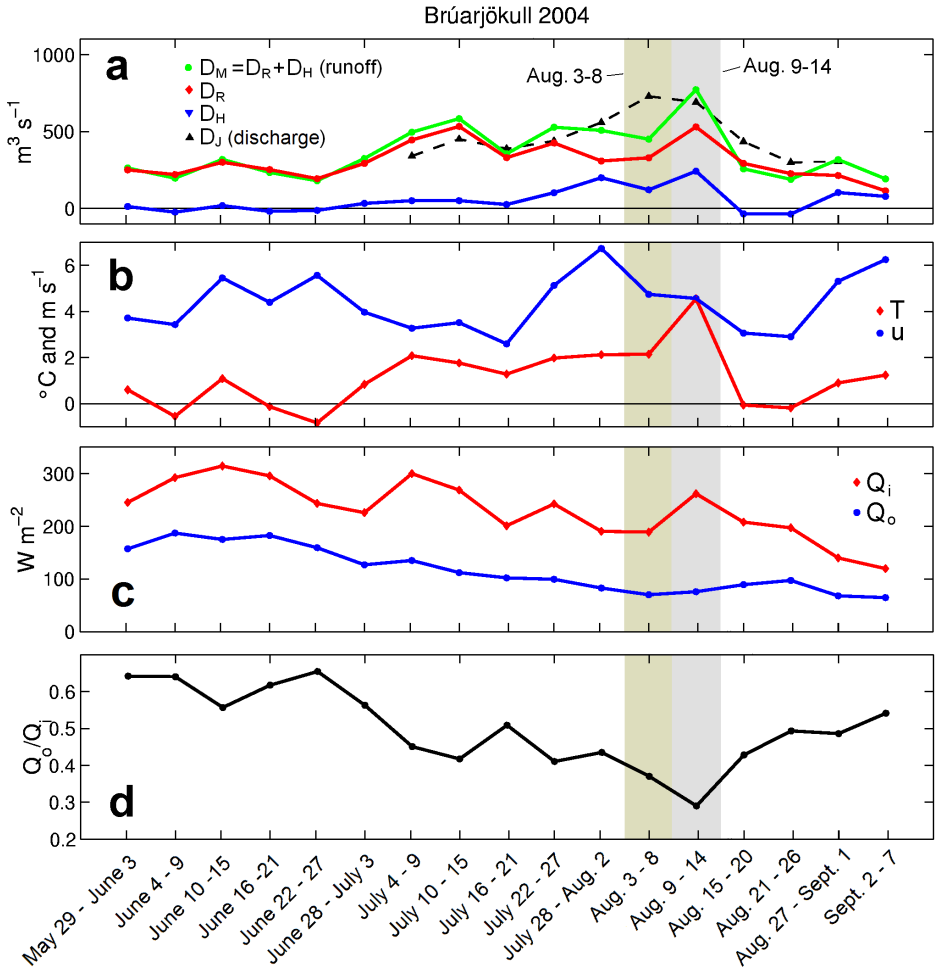



Figure 12. a) Six-day averages of the glacial runoff ($D_M$) and observed river discharge ($D_J$), 40 km north of the outlet. $D_M$ is seperated into contribution from net radiation ($D_R$) and net turbulent heat fluxes ($D_H$). b-c) Weather parameters, average of three AWSs. d) Albedo averaged over the glacier. Parameters in (b-c) are defined on p. 124. – *Heildarrennsli Jöklu borið saman við jökulþátt rennslisins og veðurþætti á Brúarjökli.*

net radiation gave high net energy and hence melting within the ablation areas (255-320 Wm$^{-2}$ at areas below the ELA). Within the accumulation zone (around 1200 to 1550 m), the air temperature inversion above the ELA resulted in net energy supplied for melting of 150 Wm$^{-2}$ at 1200 m up to 170 Wm$^{-2}$ at 1500 m, i.e. increased melting with higher elevation (August 9–14 in Figure 5).

**Runoff from Brúarjökull and discharge of Jökla 2004**

The glacial runoff toward Jökla is calculated as

$$D = \int_S a_s dS \,, \qquad (3)$$

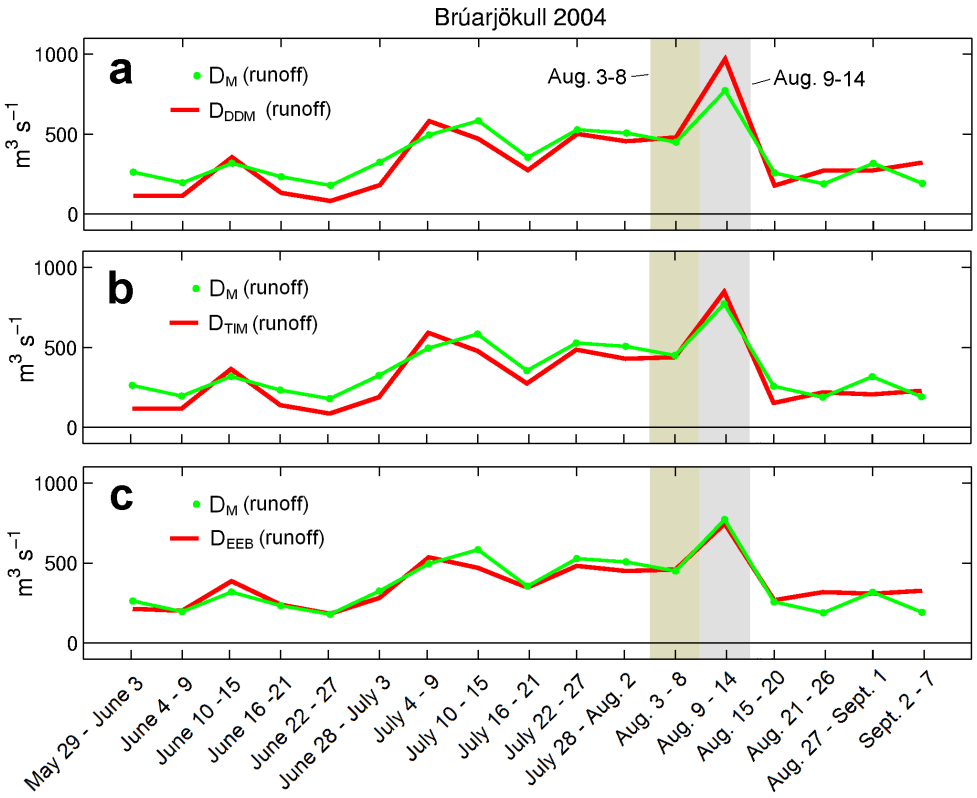



Figure 13. Six-day averages of the glacial runoff ($D_M$) as estimated from energy budget maps (from Figure 12a) compared to the runoff $D_{DDM}$ (a), $D_{TIM}$ (b) and $D_{EEB}$ (c) calculated by Eq. (3) with $a_s$ from Eqs. (4-6), respectively. – *Afrennsli frá jökli, metið út frá orkubúskap og reynslubundnum líkönum.*

where $S$ is the glaciated area of the water drainage-basin of the river (Figure 1). The glacial melting ($a_s$) was derived by Eq. (2) with $M_c$ from the energy budget maps and Eq. (3) used to compute the glacial runoff ($D_M$). Results were compared with the observed daily river discharge ($D_J$) and average weather components and surface characteristics on the glacier (Figure 12). Typical delay time between the daily glacial melting peak in ablation areas and the corresponding discharge peak of the outlet glacier have been estimated to be ∼4 hours (e.g. Rist, 1983). During the ablation season, the main contribution to glacial runoff was due to net radiation that followed the incoming solar radiation and albedo (Figure 12). During the first part of the ablation season, the contribution from the turbulent heat fluxes was close to zero, but glacial runoff became more influenced by these heat fluxes during a warm and windy period from mid-July to mid-August. Of special interest is the period from July 28 to August 14 (before and during the floods in Jökla), which we separate into three phases:

1. A period of exceptionally strong winds from July 28 to August 1 with high turbulent heat fluxes, and low net radiation due to low solar radiation (Figures 12a-c and 3e). The average

river discharge of Jökla (550 $m^3s^{-1}$) could be explained by glacial melting, 60% of which was due to the net radiation and 40% from the high turbulent heat fluxes (Figure 12a).

2. The first flood in Jökla, August 3–6, when only ∼65% of the average river discharge (750 $m^3s^{-1}$) could be explained by glacial melting (Figure 12a); 72% of the melting was contributed by the net radiation and 28% by the turbulent heat fluxes. Thus, ∼35% of the river discharge was due to the intensive rainfall during August 1-3 (Table 1).

3. The second flood in Jökla, August 9-14, when the average river discharge (690 $m^3s^{-1}$) could be fully explained by the net energy supplied for glacial melting (Figure 12a). The exceptionally high temperatures and stable winds of ∼4.5 m $s^{-1}$ maintained high turbulent heat fluxes, and the high solar radiation, along with abruptly reduced albedo, led to strong net radiation (Figure 12). The contribution from the net radiation was 69% while 31% came from the turbulent heat fluxes.

Table 1: Accumulated precipitation at Akurnes during August 1–4, 2004 (see Figure 1 for location). – *Úrkoma á Akurnesi dagana 1.–4. ágúst 2004.*

| Time interval dd.mm hh:mm | $P_s$ mm of water |
|---|---|
| 31.07 09:00 – 31.07 18:00 | 0 |
| 31.07 18:00 – 01.08 09:00 | 0.5 |
| 01.08 09:00 – 01.08 18:00 | 21.5 |
| 01.08 18:00 – 02.08 09:00 | 25.5 |
| 02.08 09:00 – 02.08 18:00 | 2 |
| 02.08 18:00 – 03.08 09:00 | 64.7 |
| 03.08 09:00 – 03.08 18:00 | 12 |
| 03.08 18:00 – 04.08 09:00 | 0 |

**Runoff estimated from empirical models**

Three empirical ablation models were considered relating the daily ablation ($a_s$ in mm of water) at an elevation $h_G$ on the glacier to daily mean air temperature $T_S$ at an elevation $h_S$, 20 km away from the glacier front (at Eyjabakkar 655 m a.s.l., see Figure 1):

$$a_s = \begin{cases} ddf \cdot \hat{T}; & \hat{T} \geq 0 \\ 0; & \hat{T} < 0 \end{cases}, \tag{4}$$

$$a_s = \begin{cases} (MF + a \cdot Q)\hat{T}; & \hat{T} \geq 0 \\ 0; & \hat{T} < 0 \end{cases}, \tag{5}$$

$$a_s = \begin{cases} \dfrac{TF \cdot \hat{T} + b \cdot Q}{\rho L}; & (TF \cdot \hat{T} + b \cdot Q) \geq 0 \\ 0; & (TF \cdot \hat{T} + b \cdot Q) < 0 \end{cases}, \tag{6}$$

where $\hat{T} = (T_S + \gamma(h_G - h_S))$. The term $\gamma = -0.6 \times 10^{-2}$ °C $m^{-1}$ is a constant lapse rate and $Q$ is a theoretically calculated clear-sky irradiance (Olseth *et al.*, 1995). Eq. (4) is a degree-day model (DDM) (e.g. Jóhannesson *et al.*, 1995), Eq. (5) is the temperature-index model (TIM) introduced by Hock (1999) and Eq. (6) is an empirical energy balance model (EEB). The scaling factors, *MF* and *TF*, are assumed to be constant and $ddf$, $a$ and $b$ to have one value for snow and another for firn/ice (Table 2). The model in Eq. (5) is the same as given by Gudmundsson et al. (2003, p. 5–6) except that the long-wave radiation balance is ignored. *TF* is a turbulent heat flux scaling factor and $b$ is mainly reflecting the surface albedo (on average for snow or firn/ice) and the average cloud cover. The term $\rho L$ is the same as in Eq. (2). The advantage of Eqs. (4–6) is the use of air temperature, observed at non-glaciated area away from the glacier front, as the only input.

The coefficients of the empirical models (Table 2) were optimized for Brúarjökull by using the energy balance calculations at the AWSs (Eq. 2) from 1996-2001, and then tested for the years 2002-2004. Glacial runoff towards Jökla calculated by Eq. (3) with $a_s$ from Eqs. (4-6) ($D_{DDM}$, $D_{TIM}$, and $D_{EEB}$, respectively), was compared to glacial runoff ($D_M$) derived from the energy budget (Figure 13). Of the three models, the EEB model in Eq. (6) gave the best prediction of the total glacial runoff; it is the only model that does not underestimate the melting before mid-July,

Table 2: Coefficients of Eqs. (4-6) ($DDM$, $TIM$ and $EEB$, respectively) optimized for the whole Brúarjökull outlet (constant in time and space) by using the AWS data from 1996–2001. $i$ and $ii$: Before and after exposure of the previous year's summer surface, respectively. – *Stuðlar í reynslubundnum líkönum af leysingu jökuls.*

| | $\mathrm{ddf}_i$ mm °C$^{-1}$ | $\mathrm{ddf}_{ii}$ mm °C$^{-1}$ | MF mm °C$^{-1}$ | $\mathrm{a}_i$ mm W$^{-1}$ m$^2$ °C$^{-1}$ | $\mathrm{a}_{ii}$ mm W$^{-1}$ m$^2$ °C$^{-1}$ | TF W m$^2$ °C$^{-1}$ | $\mathrm{b}_i$ | $\mathrm{b}_{ii}$ |
|---|---|---|---|---|---|---|---|---|
| DDM | 5.7 | 6.6 | - | - | - | - | - | - |
| TIM | - | - | 2 | 0.01 | 0.015 | - | - | - |
| EEB | - | - | - | - | - | 13.9 | 0.1 | 0.24 |

when the runoff was mainly produced by the net radiation alone. Better prediction is achieved with the TIM model in Eq. (5) than the DDM in Eq. (4); unlike the degree-day factor ($ddf$) of the DDM model, the scaling factor of the TIM model accounts for the reduced solar zenith angle, and hence gives a better prediction during the latter parts of the ablation season (Figure 13a,b). None of the three empirical models accounts for wind-speed changes, but all predict runoff reasonably from July 28 to August 2, when intensive windspeeds, and hence high turbulent heat fluxes, were observed on the glacier (Figures 3b,c,d,f and 12b). This can be explained by low net radiation compensating for the strong turbulent heat fluxes (Figures 12 and 3e).

## CONCLUSION

Meteorological observations within the boundary layer of Brúarjökull, along with mass balance measurements at stakes, were successfully used to create energy budget maps for the ablation season during 2004. The energy budget maps effectively estimate glacial runoff, and are in good agreement with the observed river discharge of Jökla, which drains the outlet. The flood that occurred during the period August 3-6 was related to exceptionally intensive rain, but glacial melting caused the flood that occurred from August 9-14. The circumstances leading to the second flood were i) five days with high turbulent heat fluxes driven by strong southerly winds (July 28 to August 1) and heat supplied by rain (August 1–6), all speeding up the removal of snow in the ablation area and lowering the albedo, and ii) exceptionally high air temperatures and solar radiation along with abruptly reduced albedo (August 9-14).

Seasonal variations in glacial runoff during 2004 can be calculated by three empirical ablation models, which use air temperature observed away from the glacier front as the only input. The best result was obtained using an empirical energy balance model, especially during periods when melting was maintained by the net radiation alone. The glacial peak-runoff during the second flood was predicted acceptably by both an empirical energy balance- and a temperature index model that accounts for changes in the solar zenith angle by incorporating theoretically calculated clear-sky irradiance. A simple degree-day model, not accounting for changes in the solar radiation, predicted the second flood but overestimated the glacial peak-runoff. The simplicity of the empirical models is a great advantage. Air temperature away from glacier is easier to assess than weather parameters on the glacier needed for the energy balance calculations. However, the empirical models do not provide the same detailed insight into the physical processes generating the glacial runoff.

**Acknowledgements**

The work was supported by the National Power Company of Iceland, the University of Iceland Research Fund and the Nordic project Climate, Water and Energy. We are indebted to Einar Sveinbjörnsson at the Icelandic Meteorological Office for supplying data and assisting with interpretation of meteorological data and optical satellite images, and Amy E.

Clifton for constructive comments on the manuscript. Critique from three reviewers greatly improved the manuscript.

## ÁGRIP

**Orkubúskapur á Brúarjökli og orsakir stórflóða í Jöklu í ágúst 2004**

Sjálfvirkar veðurstöðvar hafa verið reknar á Brúarjökli síðan 1994, í þeim tilgangi að mæla orkustrauma sem berast að yfirborði jökulsins og valda leysingu. Niðurstöður mælinganna hafa stóraukið skilning á orsakaþáttum leysingar og tengslum hennar við veðurfar, vetrarákomu og yfirborðseiginleika jökulsins.

Tvö stórflóð urðu með skömmu millibili í Jöklu í ágúst 2004. Það fyrra varði frá 3.–6. ágúst og fylgdi í kjölfarið á mikilli úrkomu á suðaustur hluta landsins. Ljósmyndir frá gervitunglum benda til að úrkoman hafi náð hámarki á þeim svæðum Brúarjökuls sem tilheyra vatnasviði Jöklu. Veðurmælingar á jökli sýna ennfremur að heildarorka til leysingar var lítið meiri en í meðalári og að 65% af rennsli í Jöklu orsakaðist af jökulleysingu og 35% vegna regnvatns. Seinna flóðið frá 9.–14. ágúst stafaði eingöngu af jökulleysingu og fylgdi óvenju hlýju lofti og heiðríkju yfir Íslandi, ásamt umtalsverðri lækkun á endurkastsstuðli sólgeislunar 9. ágúst. Óvenju mikil jökulleysing þessa daga var því viðhaldið af mörgum samverkandi þáttum. Heitur loftmassi yfir jöklinum leiddi af sér mikinn aðflutning varma með loftstraumum, sem orsakaði 31% af jökulleysingunni. Megnið af jökulleysingunni (69%) var vegna mikils geislunarvarma sem stafaði af hreinni og sterkri sólgeislun samfara óvenju lágum endurkastsstuðli. Lækkun á endurkastsstuðli má rekja til þess að vetrarsnjór hvarf af stórum svæðum á jöklinum þann 9. ágúst, en leysing vegna hlýrra og mjög hvassra suðlægra vinda 28. júlí til 1. ágúst, ásamt úrkomunni dagana þar á eftir, flýttu fyrir þeim atburði.

Annað markmið með rekstri veðurstöðva á jökli er að athuga samhengi jökulleysingar við hitastig utan jökuls. Atburðirnir í ágúst 2004 gáfu einstakt tækifæri til að prófa mismunandi reynslubundin líkön og sjá hvernig þau bregðast við óvenjulegum aðstæðum. Athuguð voru þrjú mismunandi líkön: a) einfalt gráðudagalíkan með fastri skölun fyrir snjó annars vegar og ís hins vegar, b) samskonar gráðudagalíkan sem að auki tekur tillit til breytilegrar sólgeislunar og c) reynslubundið orkubúskaparlíkan sem metur iðuvarmastrauma út frá hita utan jökuls og geislunarvarma með líkanagerðri hreinni sólgeislun og endurkastsstuðli nálguðum sem tveir fastar, annar fyrir snjó og hinn fyrir ís. Besta niðurstaðan fékkst með reynslubundnu orkubúskaparlíkani. Öll líkönin spáðu stórflóði í Jöklu 9.–14. ágúst; líkön 2 og 3 spáðu réttu rennsli í ánni, en líkan 1, sem tekur ekki tillit til breytilegrar sólarhæðar, ofmat afrennsli jökulsins.

## REFERENCES

Björnsson, H. 1972. Bægisárjökull, North Iceland. Result of glaciological investigations 1967–1968. Part II. The energy balance. *Jökull* 22, 44–61.

Björnsson, H., F. Pálsson, M. T. Guðmundsson and H. H. Haraldsson 1998. Mass balance of western and northern Vatnajökull, Iceland, 1991–1995. *Jökull* 45, 35–58.

Björnsson, H. F. Pálsson and H. H. Haraldsson 2003. Mass balance of Vatnajökull (1991–2001) and Langjökull (1996-2001), Iceland. *Jökull* 53, 75–78.

Björnsson, H., S. Guðmundsson and F. Pálsson 2006. Glacier winds on Vatnajökull ice cap, Iceland, and their relation to temperatures of its lowland environs. *A. Glaciol*. 41, in press.

Greuell, W. and C. Genthon 2003. *Mass Balance of the Cryosphere: Observations and Modelling of Contemporary and Future Changes*, eds. Jonathan L. Bamber and Antony J. Payne. Published by Cambridge University Press. Cambridge University Press.

Guðmundsson, S., H. Björnsson, F. Pálsson and H. H. Haraldsson 2003. Comparison of physical and regression models of summer ablation on ice caps in Iceland. Science Institute, University of Iceland, report *RH-15-2003*, 33 pp. Available at: http://www.raunvis.hi.is/∼sg/emodels.pdf

Hock, R. 1999. A distributed temperature-index ice- and snowmelt model including potential direct solar radiation. *J. Glaciol*. 45(149), 101–111.

Hólm, S. L. and H. Sigurjónsson 2004. Runoff forecast for the river Jökulsá á Dal, August 2004. Vatnaskil Consulting Engineers. Prepared for the *National Power Company* in Iceland, 55 pp.

Jóhannesson, T., O. Sigurðsson, T. Laumann and M. Kennett 1995. Degree-day mass balance modelling with

applications to glaciers in Iceland, Norway and Greenland. *J. Glaciol.* 41(138), 345–358.

Oerlemans, J. 1998. The atmospheric boundary layer over melting glacier. In: *Clear and Cloudy Boundary Layers* (eds. A. A. M. Holtslag and P. G. Duynkerke), Royal Netherlands Academy of Arts and Sciences, Olace, VNE 48, ISBN 90-6984-235-1, 129–153.

Olseth, J. A., A. Skartveit and H. Zou 1995. Spatially continuous mapping of solar resources in a complex high latitude topography. *Solar Energy* 55, 475–485.

Pálsson, F., H. Björnsson, E. Magnússon and H. H. Haraldsson 2004. Vatnajökull: Mass balance, meltwater drainage and surface velocity of the glacial year 2003-2004. Science Institute, University of Iceland, report *RH-23-2004*, 37 pp.

Rist, S. 1983. Floods and flood dangers in Iceland. (Flóð og flóðahætta). *Jökull* 33, 119–132.

van den Broeke, M. R. 1997. Momentum, heat and moisture budgets of the katabatic wind layer over a midlatitude glacier in summer. *J. Appl. Meteorol.* 36(6), 763–774.